Tensile properties improvement of a unidirectional-mat flax/epoxy composite via click chemistry, nanocellulose addition and surface refining of short mat fibres

Abdelhadi Blal[1], Gilbert Lebrun[1,2*], François Brouillette[1,3], Éric Loranger[1,2]

[1] Innovations Institute in Ecomaterials, Ecoproducts and Ecoenergies, Biomass-based (I2E3), Université du Québec à Trois-Rivières (UQTR)

[2] Department of Mechanical Engineering, Université du Québec à Trois-Rivières (UQTR)

[3] Department of Biochemistry, Chemistry, Physics and Forensic Sciences, Université du Québec à Trois-Rivières (UQTR)

* To whom correspondence should be addressed

Abstract

The mechanical characteristics of natural fibre composites (NFCs) are closely linked to fibre-matrix and fibre-fibre interactions. This work investigates the improvement of tensile properties of a flax/epoxy composite through the application of click chemistry reaction to a unidirectional-mat (UDM) reinforcement with modifications made on the short fibre mat and unidirectional flax fibre phases of the reinforcement. The surface of short flax fibres was fibrillated to increase the accessibility of hydroxyl groups for all preliminary reactions and the final click chemistry cross-linking, which creates stable covalent triazole bonds between azide and alkyne groups. A small percentage of treated nanocellulose was incorporated to further enhance the reinforcement properties. FTIR and EDX analysis confirmed the presence of the various functional groups on the surface of nanocellulose and flax fibres with very high degrees of substitution. The treatment significantly improved the mechanical properties of the dry reinforcement, including a 220% mean increase in the tensile strength. However, the treatments, particularly the addition of nanocellulose, resulted in a reduction in the permeability to liquid resin of the reinforcements, highlighting the need for compromises in their manufacture. Nonetheless, marked improvements in tensile strength and Young's modulus were obtained for composites made of pre-compacted and cross-linked fibre preforms. Increases in elastic modulus, strength and strain at break of up to 50.1%, 53.8% and 10.1% were obtained, respectively.

Keywords: Flax/Epoxy composites, Click Chemistry, Fibrillation, Nanocellulose, Tensile testing

1. INTRODUCTION

In recent years, the shift towards sustainable development has intensified the search for environmentally friendly materials that do not compromise performance. Because of their interesting properties, natural fibre composites are increasingly used in various sectors such as automotive, construction, aerospace, and electrical engineering [1]. Like most natural fibres, flax offers a renewable alternative to synthetic fibres with the added benefits of a low density, high strength-to-weight and stiffness-to-weight ratios, and lower carbon footprint [2]. In the composites industry, flax fibres are valued for their potential to create strong materials, a crucial characteristic in many industries like transportation and aerospace [3]. Despite their promising attributes, flax fibres face inherent challenges that limit their application in demanding environments. These include lower mechanical strength and modulus compared to synthetic fibres, as well as a natural tendency to absorb moisture, which adversely affects their compatibility with hydrophobic polymer matrices such as epoxy [4]. This incompatibility often leads to poor interfacial adhesion, a critical factor for the mechanical properties of composites. Moisture sensitivity can also induce swelling and microbial degradation, further compromising the long-term integrity of the material. In consequence, enhancing the surface properties of natural fibres through mechanical or chemical treatments is essential to improve interfacial adhesion and directly impact the mechanical performance and durability of the composite [5-8].

Typical mechanical treatments, such as fibrillation, increase the surface area of fibres, allowing an increased mechanical interlocking with the matrix. This process not only enhances the fibre-matrix adhesion, but also improves the distribution of stress within the composite, leading to higher strength and toughness [9-12]. Fibre preform compaction compresses the fibre bed to promote fibre-fibre contact thereby improving the mechanical properties of composites [13]. Other mechanical treatments, such as electron beam [14] and gamma rays [15], can also improve the properties of natural fibre composites. However, mechanical treatments alone fall short in tackling specific challenges, such as the hydrophilic nature of natural fibres and their vulnerability to environmental degradation [16]. To overcome these limitations, a wide range of chemical treatments have been extensively investigated [17]. For instance, alkaline treatment can remove lignin, hemicelluloses, and other fibre impurities, increasing the surface roughness while exposing more cellulose reactive hydroxyl groups [18, 19]. This treatment often improves interfacial bonding between the fibres and matrix, thus enhancing the composite strength and stiffness [20, 21]. Acetylation involves treating fibres with acetic anhydride, substituting hydroxyl with acetyl groups on the fibre surface. By reducing the hydrophilicity of fibres, acetylation decreases moisture absorption and enhances the compatibility with hydrophobic polymer matrices to provide improved

dimensional stability and mechanical properties [22, 23]. Silane coupling agents, like 3-aminopropyl triethoxysilane, can form a molecular bridge between the fibres and the polymer matrix by hydrolysis of the silane compound to form silanol groups that can react with hydroxyl groups on the fibre surface [24, 25]. This significantly enhances the interfacial adhesion, mechanical properties and hydrophobicity in flax fibres-based composites [26] and in sisal fibres reinforced PLA [27]. Surface of fibres can also be oxidized to introduce functional groups such as carboxyl and carbonyl groups. This process increases the surface roughness and fibre reactivity, improving the fibre-matrix adhesion, leading to an increase in tensile strength of 106% by improving the interfacial adhesion strength to 532% [28]. Finally, other chemical treatments, including benzoylation [29, 30], peroxide [31], and isocyanate [32], can improve the fibre-matrix compatibility by introducing reactive sites that can form covalent bonds [4, 33-36]. However, these treatments often have drawbacks such as requiring harsh reaction conditions, and the potential for incomplete reactions, which can limit their effectiveness and practicality. More recently and compared to these conventional chemical treatments, advanced chemical methods like click chemistry have been increasingly considered in the development of composite materials, in particular for their high efficiency, specificity, and ability to form robust covalent bonds under mild conditions, outperforming traditional chemical treatments [37–39]. Click chemistry stands out due to its exceptional reactivity under mild conditions, often proceeding at room temperature and in aqueous media, making it more environmentally friendly and safer to handle. The reaction involves the selective formation of covalent bonds between specific functional groups, limiting unwanted side reactions and ensuring a high degree of cross-linking within the fibre network. The triazole bonds formed during this process are chemically and thermally stable, offering enhanced durability and long-term performance, which contribute to improve the mechanical properties and consistency of the final composite [40]. A high-performance cellulose nanofibre (CNF)-based composite was developed by Zhang et al. [41] through a combination of click chemistry, coordination reactions, and solvent exchange. The obtained CNF-composite exhibited excellent thermal stability below 230 °C, and its mechanical stability was achieved through the robust three-dimensional CNF-based crosslinking network created via the click chemistry process. In previous works [42, 43], it was shown that click chemistry can form fibre-fibre covalent bonds and improve the mechanical properties of kraft pulp fibre sheets and short fibre mat reinforcements. Compared to the untreated samples, the stiffness of the treated kraft sheets increased by 44%, the tensile and burst strengths by 75% and 193% respectively, and the elongation at break reached a notable increase of 111% [42]. Tests conducted on dry flax mats (short fiber mats) subjected to click chemistry and compaction showed increases of 519%, 355%, 201%, 304%, and 421% in tensile, elongation at

break, tensile stiffness, burst, and tear indexes respectively, while tensile tests on composite plates revealed improvements of 41.5% in tensile modulus, 64.3% in strength, and 30.8% in strain at break [43]. Incorporating nanoparticles (e.g., nanocellulose) in composites can further enhance surface properties by introducing nanoscale features improving the interaction between fibres and matrix [44, 45].

Previous works by the authors were dedicated to the development of a unidirectional (UD) flax fibre reinforcement using kraft pulp or short flax fibres as a binder for the UD layer, commonly referred to as a UD-mat (UDM) reinforcement [46-48]. In other studies, the click chemistry reaction was applied to kraft pulp fibres only, for the fabrication of stronger paper sheets [42], and to short flax fibre mat reinforcements to enhance the properties of the dry mat and its composite materials [43]. In the present work, the same chemical treatments are applied to more compact UD-mat reinforcements to increase the tensile properties of a UD flax-epoxy composite for eventual uses in more structural applications. First, surface fibrillation is performed on the short flax fibres to expose more reactive sites, facilitating the creation of covalent bonds during the click chemistry reaction. This treatment also enhances the fibre-matrix interaction. Then, propargylation is performed on the UD fibres, azidation on the short fibres of the mat phase, so the click chemistry reaction occurs between the mat and UD phases in the UDM reinforcement. Azidated nanocellulose is also incorporated to some reinforcements before molding to evaluate how it can contribute to create more covalent bonds with UD fibres and enhance the composite properties. Its nanoscale dimensions and high surface area, combined to the surface fibrillation of the short fibres and fibre preform compaction are expected to improve the overall tensile performance of the flax-epoxy laminates.

2. EXPERIMENTAL METHODS

2.1. Materials

Flax fibres were obtained from Safilin Inc. (Szczytno, Poland). A Tex 5000 ribbon, cut into short fibres approximately 6 ± 1 mm in length, was used in the mat layer of the reinforcement, and a low twist Tex 400 yarn was used for the unidirectional (UD) layer. For the preparation of nanocellulose, the commercial bleached softwood kraft pulp was provided by Fraser Paper (Thurso, Canada). Reagents were purchased from different suppliers: propargyl bromide (80% in toluene), p-toluenesulfonyl chloride, and sodium azide (Alfa Aesar); sodium hydroxide and copper sulphate pentahydrate (Acros Organics); sodium bromide (Fisher Scientific) and dimethylformamide

(DMF), 4-acetamido-TEMPO, sodium ascorbate, and triethylamine (Sigma-Aldrich). Sodium hypochlorite (6 %v/v) was purchased from a local store. The resin system used for composite plates was composed of SikaBiresin CR72 resin mixed with SikaBiresin CH72-3 hardener at a ratio of 18 g of hardener per 100 g of resin, both supplied by Sika Advanced Resins (USA). All chemicals were used without further purification.

2.2. Preparation of nanocellulose

A nanocellulose gel (Nano-OX) was prepared from oxidized kraft pulp fibres using shear processing with an IKA defibrillation system, according to the procedure described by Lassoued et al. [49]. First, kraft pulp fibres (30 g dry) were dispersed in deionized water. Concurrently, 2.2 g of 4-acetamido-TEMPO and 5 g of sodium bromide were dissolved in a minimal volume of deionized water. This solution was then introduced into the reactor. Additional deionized water was added to adjust the total volume to 3 L at 1% consistency. The mixture was held at 25°C and pH between 10 and 11. The oxidation reaction was initiated by adding 250 mL of sodium hypochlorite and allowed to proceed for two hours. The reaction was terminated by adding 75 mL of 3% hydrogen peroxide to neutralize any remaining sodium hypochlorite. The oxidized pulp was then filtered and transferred to a Plexiglas tank connected to a defibrillation system including a pump, a defibrillator, and a bubble cooler to control the heat generated. The defibrillation process lasted two hours and resulted in the formation of a 2.5% nanocellulose gel with a carboxylate content of about 1560 mmol/kg.

2.3. Pretreatment and processing of flax fibres for the UD-mat reinforcement

A series of mechanical and chemical treatments were carried out to prepare and modify the flax fibres and nanocellulose before proceeding with reinforcement fabrication. Each intermediate chemical and mechanical treatment performed on the fibres and UD-mat reinforcement was also tested to verify its influence on the permeability to liquid resin and tensile properties of dry reinforcement, allowing the final choice for the preparation and testing of composites.

2.3.1 Alkaline pretreatment and surface fibrillation of flax fibres

The fibre pretreatment process begins with the surface fibrillation of short fibres, followed by an alkaline treatment (Figure 1). Fibrillation was performed using a Paper and Fibre Research Institute (PFI) refining mill (Noram Quality Control and Research Equipment Limited, Canada) according to the procedure described by Amir et al. [12]. 25 g dry of short flax fibres (Figure 1a) were immersed in 2 L of deionized water and soaked for at least four hours. The dispersion was then

mixed in a standard pulp disintegrator for ten minutes at 1000 rpm (Figure 1b) and fibrillation was performed in the PFI refiner (400 revolutions, 800 rpm, Figure 1c). After fibrillation, the fibres were subjected to an alkaline treatment using a NaOH solution to clean the fibres and facilitate subsequent chemical reactions. They were dispersed and stored for 24h in a 5% w/w NaOH (Figure 1d). Then, the fibres were thoroughly rinsed with deionized water, acidified water (pH around 4) to neutralize any remaining NaOH, and again with deionized water.

Figure 1. Steps in the mechanical and alkaline pretreatment process of the short flax fibres. a) Short flax fibres, b) Standard disperser, c) PFI refining mill and d) Alkaline treatment of fibrillated fibres.

2.3.2. Preparation of modified fibres and nanocellulose for the click chemistry reaction

Figure 2 illustrates the schematic representation of the chemical treatments applied to flax fibers and nanocellulose for the click chemistry reaction. Three types of flax fibers were prepared following the protocols detailed by Blal et al. [42, 43]: propargylated (FLAX-Pr), tosylated (FLAX-Ts), and azidated (FLAX-Az) fibers. Similarly, nanocellulose underwent tosylation (Nano-Ts) and azidation (Nano-Az) treatments to enable its participation in the click chemistry reaction with UD fibres. It is important to note that the nanocellulose and short flax fibres were azidated while the continuous UD fibres were propargylated. This created covalent bonds (through the click-chemistry reaction) between the short fibres and nanocellulose on one side, and the UD fibres on the other side. These treatments are summarized in the subsections below, and the reader is invited to refer to [42, 43] for further details on the experimental procedures.

Preparation of propargylated UD flax fibres (FLAX-Pr): Tex 400 flax yarns were first aligned on a flat winder made with holes (shown in the upper left corner in Figure 3) to facilitate the circulation of the reagent solutions. Propargyl bromide (230 mL) was added to 20 L of 2.5% w/v NaOH containing the flat winder with a 56 g layer of UD flax fibres. The reaction medium was left at room temperature without mechanical stirring for 10 days. Then, the mixture was diluted with 2 L of deionized water, left to rest for 4 hours, and the fibres washed with 2 x 10 L of hot water and 4 L of hot ethanol 95%.
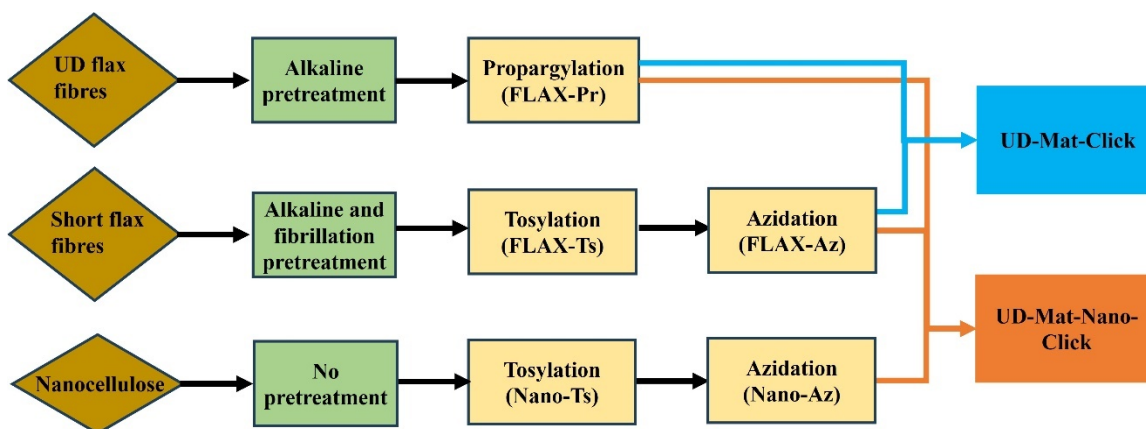
Figure 2. Experimental flowchart of flax fiber and nanocellulose treatments.

Preparation of tosylated short flax fibres (FLAX-Ts): Triethylamine (83 mL) and tosyl chloride (110 g) were added to 3 L of a dispersion containing 12 g of the short, pretreated flax fibres in 2.5% w/v NaOH and left under mechanical stirring at room temperature for 10 days. The mixture was then diluted with 2 L of deionized water and the fibres were filtered, washed with 3 x 1 L of hot water and 2 L of hot ethanol 95%, and stored in a desiccator.

Preparation of azidated short flax fibres (FLAX-Az): Sodium azide (27 g) was added to 12 g of tosylated flax fibres dispersed in 2 L of DMF and left under magnetic stirring at 75°C for 10 days with a condenser to prevent evaporation. After cooling, the mixture was diluted with 2 L of deionized water. The fibres were filtered and washed with 2 L of hot water and 2 L of hot ethanol 95% and stored in a desiccator. The 10 days reaction time for propargylated, tosylated and azidated fibres was chosen based on our recent work on short flax fibres [43]. We observed that it was necessary to increase the reaction time from 7 days for short kraft pulp fibres [42] to 10 days for short flax fibres. This extended duration was found to increase the degree of substitution in flax fibres, which require longer reaction times compared to kraft pulp fibres due to their structure and composition. For sure, such treatment durations may present challenges for high volume productions required in some industries. So future works will be required to optimize the reaction time while maintaining high functionalization efficiency to address this limitation.

Preparation of tosylated nanocellulose (Nano-Ts): Triethylamine (52 mL) and tosyl chloride (72 g) were added to 475 mL of 2.5% w/v NaOH containing 10 g of nanocellulose and let to react under mechanical stirring for 24 h at room temperature. The dispersion was then added in 500 mL of a (50-50) water/ethanol 95% mixture. The solids were filtered and washed with 500 mL of hot water and 500 mL of ethanol 95%.

Preparation of azidated nanocellulose (Nano-Az): Sodium azide (22 g) was added to Nano-Ts (8 g) dissolved in 240 mL DMF and let to react for 24 h at 75 °C. After cooling, the mixture was precipitated in 500 mL of distilled water and filtered. The precipitate was washed with 500 mL of hot water and 500 mL of ethanol 95%.

2.4. Preparation of the UD-mat flax reinforcement

Figure 3 shows the dynamic sheet former (ALIMAND Inc., France) used for the preparation of the UDM reinforcements from the short and UD flax fibres (treated or not). The reinforcements were
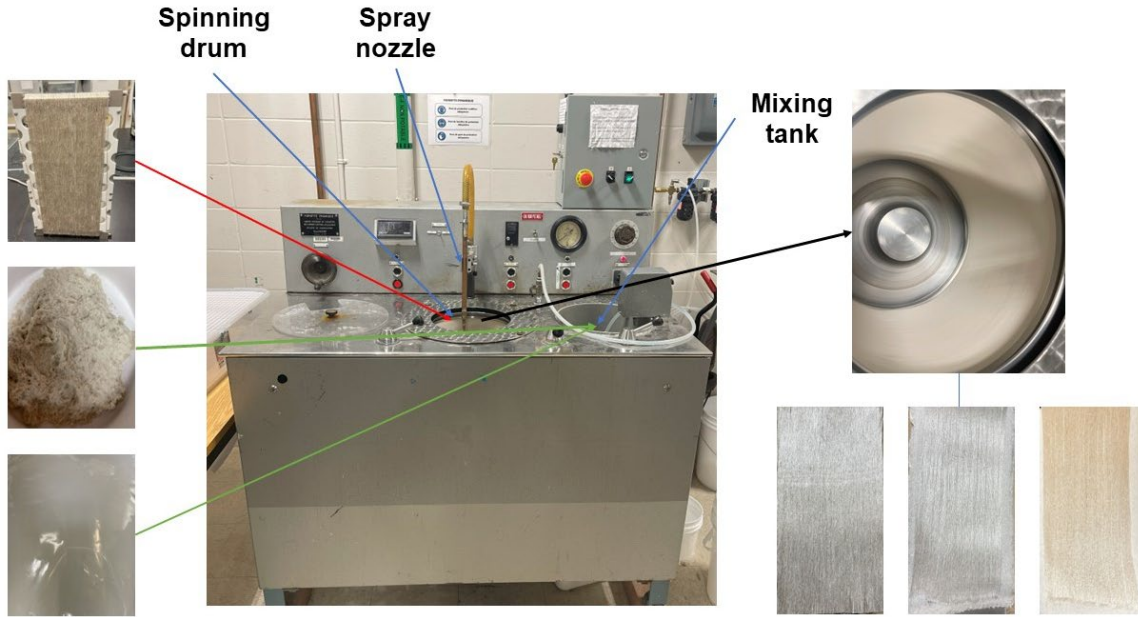

Figure 3. Dynamic former process for the preparation of the UDM flax reinforcements.

prepared following a procedure described in previous works [12, 13]. The UDM is composed of a UD layer (~250 g/m²) and a mat binder (~50 g/m²), for a total surface density of around 300 g/m². Several UDM reinforcements containing different treated fibres and additives were prepared for dry testing as listed in Table 1. After forming under wet conditions, the reinforcement is carefully removed forming drum (spinning drum in Figure 3) and dried at 110°C for 15 minutes using an E-100 drum dryer (Adirondack Machine Corporation, Hudson Falls, NY, USA). UDM3, 4, 10 and 14 were also compressed at 2.2 MPa for 5 minutes at 100°C using a 50-ton laboratory press (DAKE Corp., Grand Haven, MI, USA). The selection of pressure, time, and temperature was based on the work of Mbakop et al. [13, 48]. The reinforcements are divided into three groups: In group 1, UDM1 to UDM4 are made of untreated (UDM1, serving as reference) or mechanically treated only fibres to isolate the influence of mechanical treatments on the measured properties. In group 2, UDM5 to UDM10 are prepared with 1.5 to 9 % w/w of TEMPO-oxidized nanocellulose. The

nanocellulose was added to the short flax fibres dispersion in the dynamic former mixing tank. To compensate for incomplete retention, the required mass of nanocellulose was adjusted through a series of preliminary tests. The results of this second group of samples were then used to select the nanocellulose percentage to be used in the preparation of group 3 of reinforcements, UDM11 to UDM14. These are either combinations of conditions from the first two groups (for UDM9 and UDM10) or combinations of conditions and click chemistry (UDM11 to UDM14). The click chemistry reaction occurred during the drying step, after removing the UDM from the dynamic former.

Table 1. Nomenclature and overview of the chemical and mechanical treatments applied to various UDM reinforcements.

Type of reinforcement	Chemical and mechanical treatment
UDM1	Untreated (reference reinforcement)
UDM2	Fibrillation
UDM3	Compaction
UDM4	Fibrillation + Compaction
UDM5	Addition of 1.5% Nano-OX
UDM6	Addition of 3% Nano-OX
UDM7	Addition of 6% Nano-OX
UDM8	Addition of 9% Nano-OX
UDM9	Fibrillation + 3% Nano-OX
UDM10	Fibrillation + 3% Nano-OX + Compaction
UDM11	Fibrillation + Click reaction
UDM12	Fibrillation + Click reaction + 3% Nano-OX
UDM13	Fibrillation + Click reaction + 3% Nano-Az
UDM14	Fibrillation + 3% Nano-Az + Compaction + Click reaction

2.5. Composite plate molding

Composite plates were molded using the resin transfer molding (RTM) process, with the same mold and procedure detailed in previous works [12, 13]. Before molding, the 300 g/m^2 UDM reinforcements were dried at 70°C for 2 hours. The mold cavity thickness was adjusted using aluminium shims positioned between the mold halves to maintain a consistent fibre volume fraction (V_f) around 40% for all plates. V_f was calculated using equation (1),

$$V_f(\%) = (n \times m_{o,R}) / (h \times \rho_f) \qquad (1)$$

where n is the number of layers in the laminate, $m_{o,R}$ is the average surface density of each mat reinforcement (g/cm^2), ρ_f is the fibre density (g/cm^3) and h the laminate thickness (cm). Here, to consider the effect of fibre treatments on ρ_f (and V_f), both the fibre density of 1.44 g/cm^3 proposed by the supplier ($\rho_{f,S}$) and that measured experimentally ($\rho_{f,E}$) were considered. Flax fibre density was measured following ASTM D297 method based on Archimedes' principle. Considering the high sensitivity of flax to water (rapid water absorption), hydrophobic Canola oil ($\rho = 0.917$ $g/cm3$) was used to measure the submerged weight of fibres [50, 51].

After mixing the hardener with the resin, the mixture was degassed under vacuum for 10 minutes to remove any entrapped air. The mold containing a stack of 8 layers of reinforcements, all oriented at 0° ($[0_8]$ stacking sequence) was preheated to 80°C for 15 minutes to reduce resin viscosity and facilitate impregnation. Once the resin mixture was degassed and the mold preheated, the pressure pot was connected to the mold and slowly pressurized to 4 bars for the injection, taking care to avoid fibre displacement at the mold gate. After filling, the mold was transferred to the oven for curing. The resin was cured at 80°C for 4 hours, followed by a post-cure at 100°C for 3 hours to ensure complete cross-linking. The results of the average density (based on ten repetitions) are presented in Table 2 and the characteristics of the composite plates, such as the reinforcement type, fibre volume fraction, plate thickness and the composite porosity are detailed in Table 3.

Table 2. Density measurements of flax fibre (ten measurements).

Flax fibres Type	Density (g/cm^3)
Untreated	1.41 ± 0.03
Fibrillated	1.40 ± 0.02
Click chemistry	1.45 ± 0.04
Propargylated	1.37 ± 0.03
Azidated	1.47 ± 0.08
NaOH pretreated	1.37 ± 0.04

Table 3. Characteristics of composite plates made of different UDM reinforcements.

Composite plate	Reinforcement type	V_f calculated from $\rho_{f,S}$ (%)	V_f calculated from $\rho_{f,E}$ (%)	Plate thickness, t (mm)	Plate porosity (%)
C1	UDM1	39.8 ± 0.1	40.5 ± 0.1	4.03 ± 0.45	2.2 ± 0.5
C2	UDM2	38.8 ± 0.3	39.7 ± 0.3	4.15 ± 0.37	2.4 ± 0.3
C3	UDM9	41.8 ± 0.4	42.9 ± 0.4	3.85 ± 0.24	6.3 ± 1.8
C4	UDM10	40.7 ± 0.2	41.7 ± 0.2	3.95 ± 0.47	4.8 ± 0.9
C5	UDM11	41.5 ± 0.2	41.3 ± 0.2	3.88 ± 0.05	7.3 ± 2.6
C6	UDM12	40.2 ± 0.1	40.0 ± 0.1	4.13 ± 0.18	6.1 ± 0.4
C7	UDM13	42.3 ± 0.3	42.0 ± 0.3	4.13 ± 0.36	6.2 ± 0.9
C8	UDM14	40.0 ± 0.2	39.8 ± 0.2	4.23 ± 0.17	7.8 ± 0.8

The reinforcements chosen for the plates allowed to evaluate and compare the effects of each treatment on the final properties of the composites. The low influence of the treatments on the fibre density results in fibre volume contents all around 40%, except for C7 with a value slightly higher at 42%. Thus, and considering the standard deviations, fibre treatments had no significant effect on Vf. Porosity was calculated from the volumes of resin and reinforcement in each plate, obtained by dividing their weight by their respective density. Comparing the sum of these volumes to the volume of the molded plate allowed to estimate the plate porosity. As observed, porosity is quite high for tests C3 to C8, especially for C8 at 7.8%. This point will be discussed when comparing the permeability data with the tensile tests results.

2.6. Characterization of fibres, reinforcements and composite plates

Treated fibres, reinforcements and composites were characterized using chemical analysis (on treated fibres), permeability tests (on dry reinforcements), porosity tests (on composites) and tensile testing (on dry reinforcements and composites). The chemical analysis was realized to confirm the successful propargylation, tosylation, and azidation of kraft pulp and flax fibres as previously demonstrated [42, 43]. Permeability and tensile tests performed on dry UDM reinforcements provided insights into the effects of treatments and nanocellulose incorporation on the molding and on reinforcement themselves, helping to select the reinforcements for the molding composite plates. Finally, tensile tests on composite plates allowed to evaluate the effect of the different treatments on the final properties of composites, with particular attention to the combined effect of click chemistry and mechanical treatments.

2.6.1. Chemical characterization

Infrared spectroscopy was performed using a Thermo Scientific Nicolet iS10 FTIR spectrometer, with 32 acquisitions at room temperature and a resolution of ± 4 cm^{-1}. These tests allowed to identify the functional groups introduced onto the flax fibres and nanocellulose surface. Scanning electron microscopy (SEM) assessed the effect of click chemistry and its precursor chemical treatments on fibre morphology. SEM images were obtained using a Hitachi SU1510 microscope operating in secondary electron mode with a beam current of 100 mA and an accelerating voltage of 15 kV. The microscope was equipped with an energy-dispersive X-ray spectroscope (EDX, Oxford Instrument X Max 20 mm²) for a detailed elemental analysis of the fibre surface. To enhance the SEM image quality and facilitate EDX analysis, fibres were sputter-coated with gold. This involved preparing a pellet-like compact sample from the treated fibres, which was then coated with a thin layer of conductive metal to prevent charging effects, ensuring accurate imaging and analysis. EDX analysis data complemented the FTIR findings, providing evidence of successful modifications. The functional groups on the surface of propargylated, tosylated, and azidated fibres mainly comprised carbon, sulphur, nitrogen, and oxygen.

2.6.2. Tensile testing of UDM reinforcements

Tensile tests were conducted on dry UDM reinforcements on samples measuring 25 mm by 150 mm to evaluate the tensile stiffness (TS), strain at break (SAB), and maximum force per unit width (FUW). These tests were performed following TAPPI T 494 om-01 test method using an Instron-U150 LM equipped with a 10 KN load cell, at a constant speed of 2 mm/min. Six (6) samples were tested per reinforcement type in Table 1.

2.6.3. Permeability measurement of UDM reinforcements

The planar permeability of UDM reinforcements was measured using the radial flow method, allowing measurements in both the longitudinal (UD fibre direction) and transverse directions. A 20W-50 grade motor oil, chosen for its hydrophobic nature and low viscosity (440 mPa-s at 21°C), was used to mimic the liquid epoxy resin. The test sample consisted in a stack of five layers of reinforcement, each 140 mm by 140 mm, centrally perforated with a 12 mm diameter hole serving as injection cavity. The evolution of the flow front was recorded on video and transformed into a sequence of images taken at one-second intervals. Measurements of the Rx and Ry radii derived from the ellipses allowed the determination of permeability in the longitudinal (Kx) and transverse (Ky) directions following the well-known procedure [52]. Three (3) tests were realized per reinforcement type in Table 1.

2.6.4.   Tensile testing of composites

Tensile tests were conducted in compliance with ASTM D3039 for tension testing of polymer matrix composite materials. At least five (5) tests were realized per composite plate in Table 3. Coupons 254 mm long per 25,4 mm wide were tested with an Instron-U150 LM testing machine, equipped with a 50 kN load cell. The axial extension was measured with a 50 mm Instron 2620 extensometer. The tests were conducted at a constant velocity of 2 mm/min, adhering to the standard specifications.

3.   Results and discussion

3.1.   Characterization of modified fibres and nanocellulose

3.1.1.   FTIR spectroscopy analysis

The FTIR spectra of untreated and modified flax fibres show the different functional groups added after propargylation, tosylation and azidation reactions (Figure 4). The broad peak around 3400 cm^{-1}, attributed to O-H stretching related to alcohol group, is observed in all samples, but more intensely in the NaOH, Pr, and Az treated fibres suggesting changes in hydrogen bonding and the removal of contaminants. The peaks near 2900 cm^{-1}, also found in all samples, corresponds to C-H stretching. Flax-Pr shows a new peak around 2108 cm^{-1} attributed to C≡C alkyne stretching, confirming the addition of propargyl groups. Flax-Az shows an absorption peak at 2037 cm^{-1}, characteristic of N=N=N azide stretching, verifying the presence of azide groups.
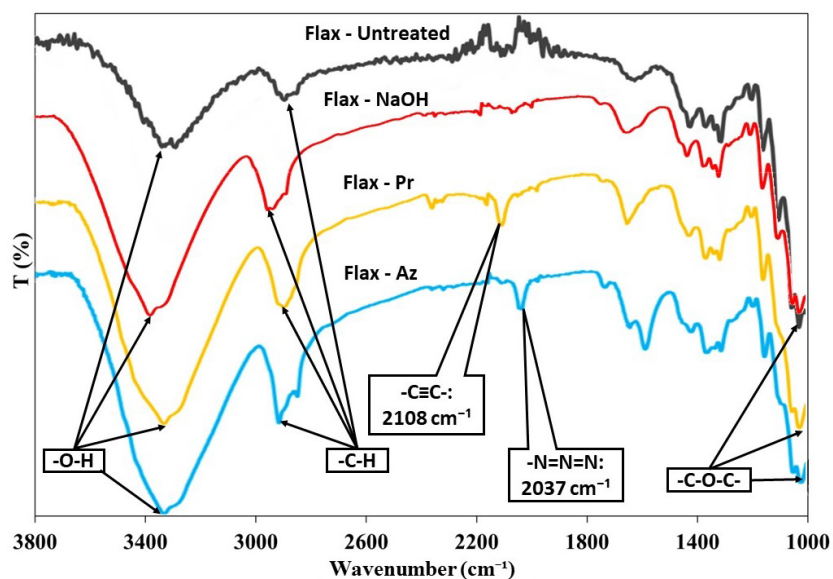

Figure 4. FTIR spectra of flax fibres with different chemical modifications, in particular –N$_3$ (azide group) for azidated fibres and –C≡C– (alkyne group) for propargylated fibres.

In Figure 5, the FTIR spectra of oxidized and modified nanocellulose (Nano-OX, Nano-Ts and Nano-Az) provide a clear contrast between the chemically modified nanocellulose gels. The spectra reveal the characteristic peaks of the functional groups introduced during the chemical modifications. For Nano-OX, the broad peak around 3300 cm^{-1} corresponds to hydroxyl groups and the peak at 1600 cm^{-1} to carboxylate groups from the oxidation of kraft pulp fibres. The Nano-Ts spectrum shows -S=O peaks around 1137 cm^{-1} and 1336 cm^{-1}, confirming the tosylation process. Azidation is confirmed by a strong sharp peak at 2045 cm^{-1}, not present in untreated nanocellulose.
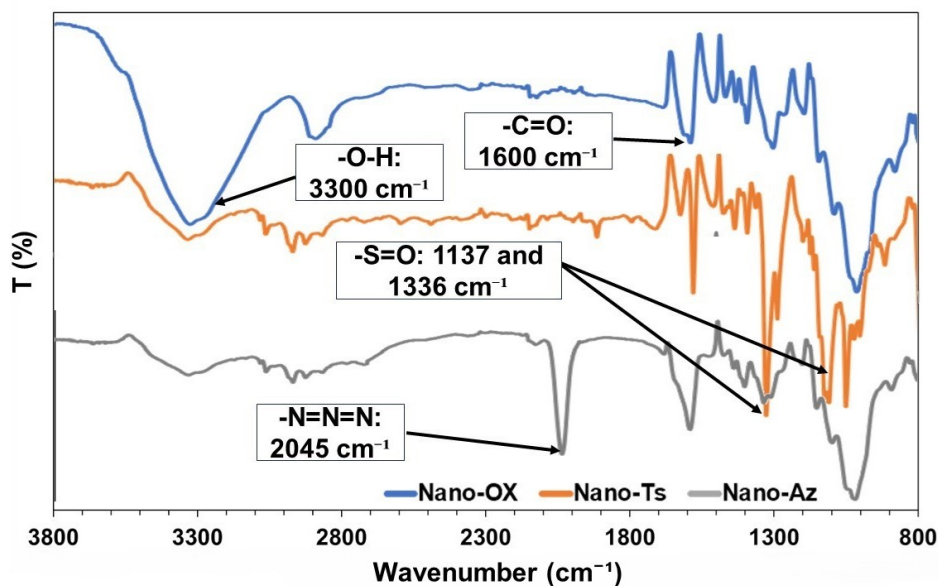

Figure 5. FTIR spectra of chemically modified nanocellulose, showing key absorption bands such as –C=O for carboxylated (by oxidation) nanocellulose, –S=O for tosylated nanocellulose, and –N$_3$ for azidated nanocellulose.

3.1.2. SEM and EDX elemental analysis

Table 4 presents the elemental composition and surface degree of substitution (DS) of the modified flax fibres and nanocellulose, as determined by EDX analysis. Notable changes occurred during the modification process reflecting the introduction of the desired functional groups and the success of the chemical treatments. Untreated flax fibres contain 65.4% carbon and 34.4% oxygen for an O/C ratio of 0.53. After the NaOH treatment, the fibres surface is relatively smooth with a homogeneous distribution of carbon and oxygen (Figure 6a). The O/C ratio increases to 0.68, probably due to the removal of organic contaminants on the fibre surface. The grafting of the propargyl group in Flax-Pr is confirmed by the sharp decrease of the O/C ratio with a high S$_{DS}$ of 2.5 (Table 4), which is corroborated by the EDX mapping showing a homogeneous increase in carbon for Flax-Pr (Figure 6b). The Flax-Ts contains a very high amount of sulphur (2.8%) evenly

distributed over the surface of the fibres (Figure 6c). The high DS of Flax-Ts (2.7) and the homogeneous distribution of tosyl groups favour the azidation reaction. Flax-Az has a nitrogen content of about 4.5% (S_{DS} = 2.1), and the substitution of the carbon-rich tosyl groups by carbon-free azide groups reduces the overall carbon content relative to oxygen, thereby increasing the O/C ratio from 0.27 to 0.56. All intermediate fibres (Pr, Ts and Az) seem to have rougher surfaces compared to Flax-NaOH, probably due to extended reaction times under mechanical stirring (Figure 6b, c, d). The same trends in O/C ratios, S_{DS} and surface roughness (Figure 7) are observed for nanocellulose. In consequence, Flax-Az and Nano-Az have a similar density of azide groups on their surface available to react with the propargyl group of Flax-Pr.

Table 4. Elemental composition and S_{DS} of modified flax fibres and nanocellulose by EDX.

Sample	Element (At. %, by EDX)				O/C	S_{DS}
	C	O	S	N		
Flax-untreated	65.4	34.4	-	-	0.53	-
Flax-NaOH	58.6	40.0	-	-	0.68	-
Flax-Pr	68.3	31.5	-	-	0.46	2.5
Flax-Ts	75.8	20.5	2.8	-	0.27	2.7
Flax-Az	60.2	33.7	0.7	4.5	0.56	2.1
Nano-Ox	59.5	37.5	-	-	0.68	-
Nano-Ts	80.6	14.9	4.1	-	0.19	2.8
Nano-Az	64.2	35.2	0.2	4.0	0.55	1.9

3.2. Effect mechanical and chemical treatments on the permeability of reinforcements

The permeability values of the UDM reinforcements are shown in Figure 8, with large differences between Kx and Ky highlighting the anisotropy of the UD composite. Untreated UDM1 exhibits the highest permeability values. As observed by Bernaoui et al. [12], fibrillation (UDM2) does not significantly alter the overall permeability. Compaction (UDM3) also slightly affect permeability by reducing interfibre voids in the preform. Combining compaction and fibrillation (UDM4) leads to decreases of 29% in Kx and 25% in Ky. These results suggest that the effect of mechanical treatments is almost insignificant, except for the combination of fibrillation and compaction.

The addition of nanocellulose is detrimental to permeability. As the nanocellulose content increases from 1.5% to 9%, both Kx and Ky decrease markedly, the lowest values are obtained with UDM7 (6% nanocellulose). This reduction is likely due to nanocellulose filling interfibre voids in the preform. However, the formation of nanocellulose clusters was observed in UDM8 reversing the downward trend in permeability. When fibrillation is combined to the adding of 3% of nanocellulose for UDM-9, the permeability re-increases compared to UDM-6, while for UDM-10 including compaction the permeability is almost maintained. So, to limit the permeability reduction,
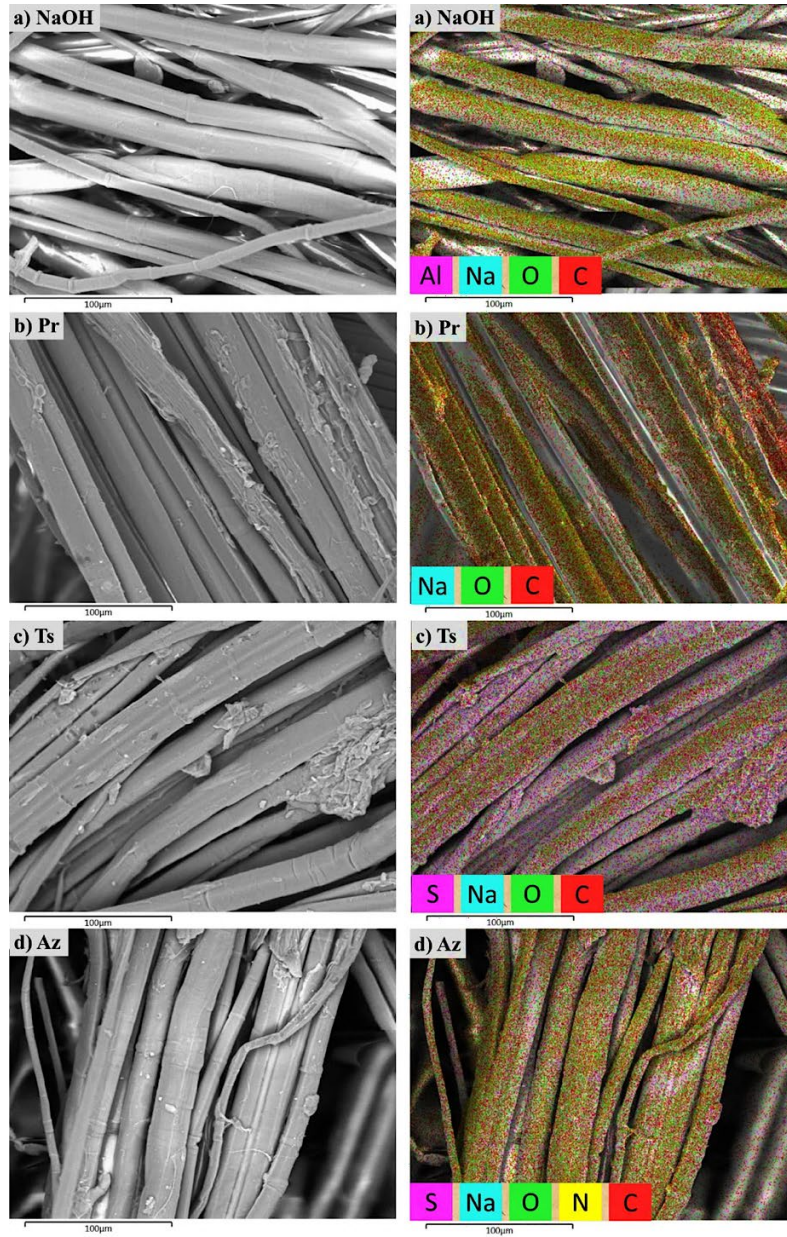

Figure 6. SEM images and EDX mapping of flax fibres: a) NaOH pretreated; b) propargylated; c) tosylated; and d) azidated.
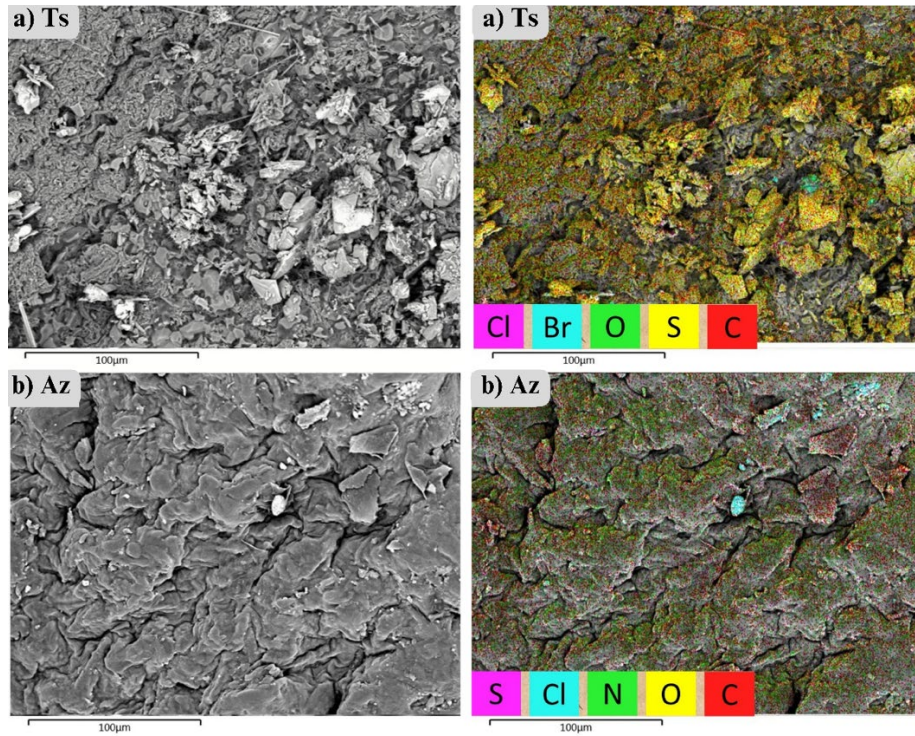
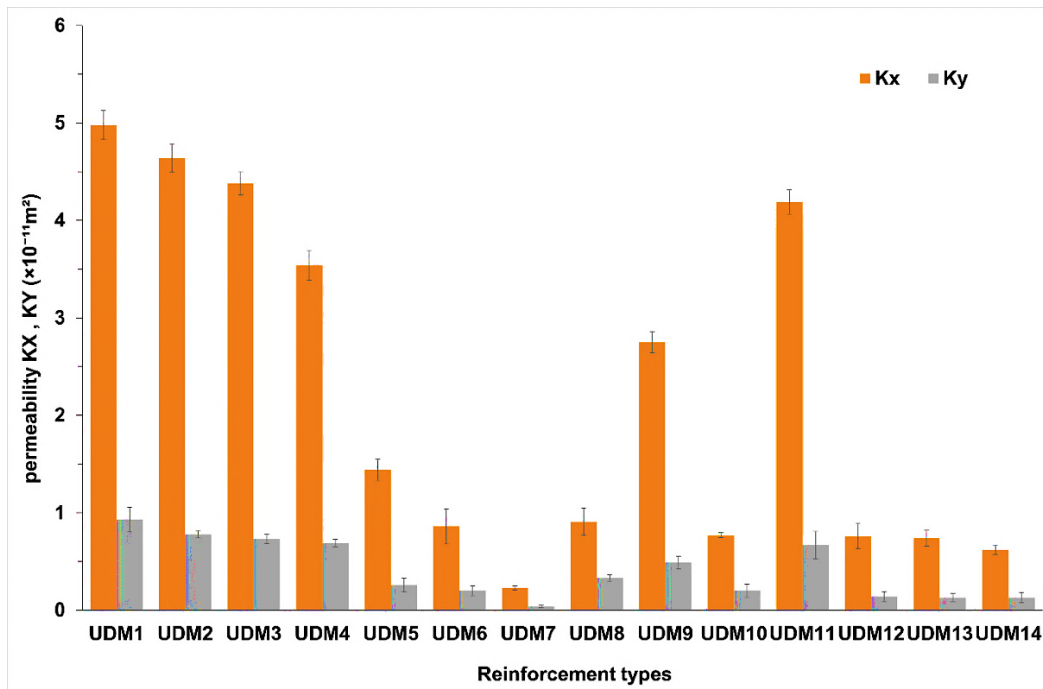**Figure 7.** SEM images and EDX mapping of nanocellulose: a) tosylated and b) azidated.

Figure 8. Impact of chemical and mechanical treatments on the permeability of UDM flax fibre reinforcements.

3% of nanocellulose is here considered a good compromise. This will be confirmed in the next section regarding the tensile tests on dry reinforcements. Reinforcements combining click

chemistry, fibrillation and compaction with 3% nanocellulose addition (UDM12 to UDM14) give low permeability values. The lowest values are observed with UDM14 ($K_x = 0.62 \times 10^{-11}$ m² and $K_y = 0.13 \times 10^{-11}$ m²). These results demonstrate the potential impact of the incorporation of nanocellulose and compaction on resin flow in the molding process. Compared to UDM11, made of fibrillated and cross-linked fibres only (no nanocellulose) and where a very small reduction in both K_x and K_y is observed compared to UDM1, this confirms the weakly negative effect of fibrillation and the strongly negative effect of adding nanocellulose.

3.3. Tensile testing of UD-mat reinforcements

The thorough testing conducted on UDM dry reinforcements is important to guide the selection of treatments for composite plate fabrication, not only in terms of ease of molding via the permeability values, but also because the increased strength and stiffness of the reinforcement will partly transfer to composite laminates. Additionally, stronger reinforcements could contribute to the preparation of geometrically consistent fibre preforms for liquid molding processes like RTM. So, it is important to examine how these treated reinforcements behave individually, which is the object of this section.

The tensile properties of UDM reinforcements described in Table 1 are presented as bar charts in Figures 9 to 11. To ease the reading and clarify the analysis, the three groups mentioned in Section 2.4 have been used. As a reminder, test UDM1 (the untreated UDM) serves as the base reference.
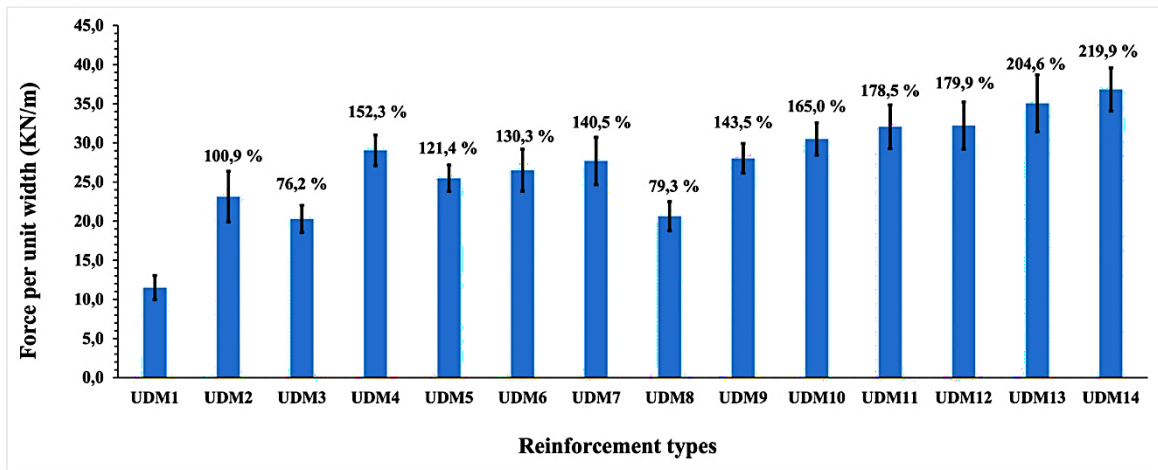

Figure 9. Force per unit width (KN/m) in the fibre direction of various UDM flax fibre reinforcements after different chemical and mechanical treatments.
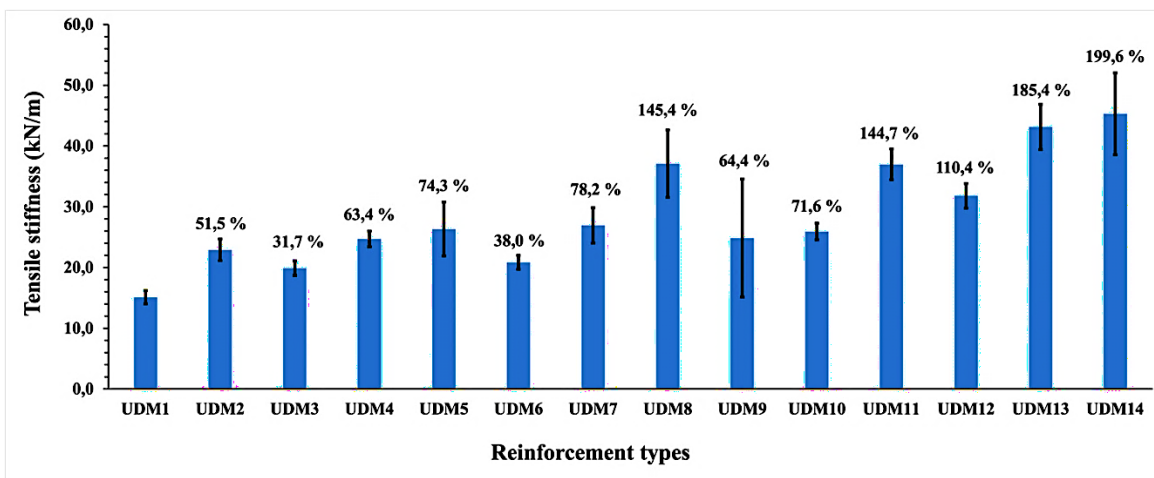
Figure 10. Tensile stiffness (kN/m) of various UDM flax fibre reinforcements after different chemical and mechanical treatments.
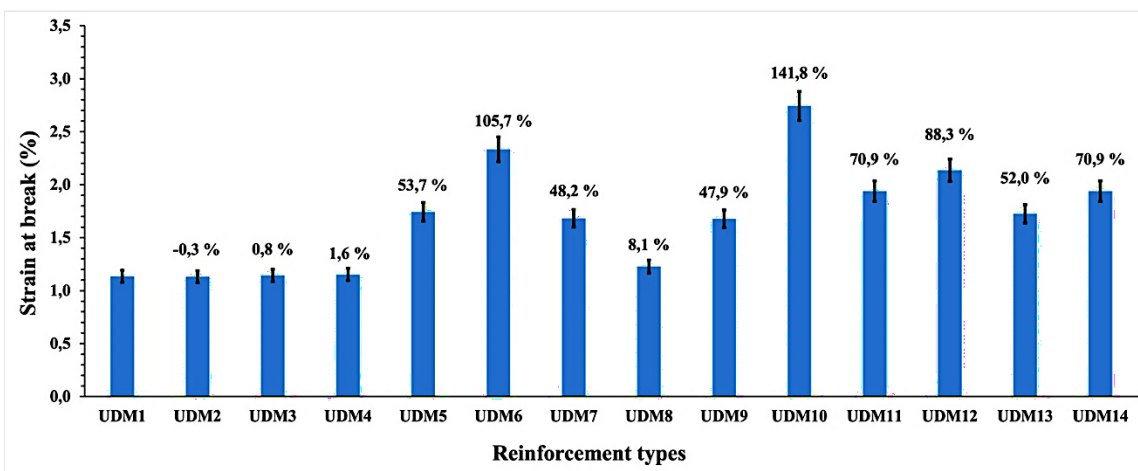

Figure 11. Strain at break (%) of various UDM flax fibre reinforcements after different chemical and mechanical treatments.

Next, UDM2 to UDM4 (group 1) correspond to tests comprising mechanically treated reinforcements only. UDM5 to UDM10 (group 2) correspond to those for which nanocellulose was added. Finally, group 3, UDM11 to UDM14 (the click treatment group), correspond to tests where the click chemistry reaction occurs between the propargylated and azidated fibres, with or without nanocellulose and reinforcement compaction. The tested properties are the force per unit width (FUW), the tensile stiffness (TS) and the strain at break (SAB). The percentages indicated correspond to the variations compared to UDM1. First, all samples show increases in FUW (Figure 9) and TS (Figure 10). Mechanical treatments of group 1, especially tests UDM2 and 3, caused lower increases in FUW and the lowest increases in TS and SAB compared to the samples of groups 2 and 3. Nevertheless, UDM2 and UDM3 show improvements of 100.9% and 76.2% in FUW and of 51.5% and 31.7% in TS compared to UDM1. These improvements are attributed to increased

interfibre contacts due to compaction and fibre entanglement promoted by fibrillation [12, 43]. However, this means that considered separately, fibrillation and compaction would be less effective at improving FUW and TS than when they are combined in UDM4 showing the highest increases of the group. They are also less effective at improving FUW and TS than when combined with nanocellulose. This is observed with the results of UDM9 and UDM10 where fibrillation is combined with compaction and the addition of 3% Nano-OX. In these samples, FUW increases up to 165.0% for UDM10, along with TS and SAB increases of 71.6% and 141.8% respectively. Comparing UDM4 (fibrillation + compaction) with UDM10 (fibrillation + compaction + 3 % Nano-OX), the adding of nanocellulose on the increase of properties seems negligible considering the variability of the results, except for the SAB where a 141.8% increase is observed for UDM10. This means adding nanocellulose has a large influence on the deformability of the dry reinforcement, so globally combining fibrillation, compaction and the addition of a low amount of nanocellulose result in significant improvement of the tensile properties.

The amount of nanocellulose that can be added depends on the results of tests containing only nanocellulose in group 2 (tests UDM5 to UDM8). The gradual addition of nanocellulose increases the FUW up to a maximum of 140.5% at 6% Nano-OX (UDM7). However, considering the very low permeability of UDM7 (Figure 8), the 130.3% improvement in FUW of UDM6 confirms the 3% adding of Nano-OX as compromise for the molding and testing of composite plates. UDM8 shows a drop in FUW due to the formation of nanocellulose clusters, as mentioned previously. There are challenges in achieving uniform dispersion at higher concentrations of nanocellulose [53]. The TS shows dropping amelioration from UDM5 to UDM6 followed by increasing effect with the nanocellulose level up to 145.4% for UDM8, while the SAB follows exactly the opposite trend in Figure 11. It shows increasing amelioration up to 105.7% for UDM6, followed by a drop down to UDM8 with only 8.1%. Again, the formation of nanocellulose clusters in UDM8 weakened the reinforcement. For this test, the relatively high FUW combined with the very low SAB resulted in the highest TS (Figure 10). Globally, UDM6 was considered a good compromise in terms of nanocellulose content for molding the composite plates because of its adequate permeability to resin combined to high FUW and SAB for the dry reinforcement.

Finally, the highest improvement in FUW and TS are obtained in group 3 after the click-chemistry reaction (UDM11 to UDM14), especially test UDM14 with mean increases of FUW and TS around 219.9% and 199.6% respectively, while SAB fluctuates around 70,9%. The direct influence of click chemistry is highlighted by comparing tests UDM10 and UDM14. Both include fibrillation, nanocellulose, and compaction; however, UDM14 also incorporates click chemistry. Very high

improvements are observed in Figures 9 to 11 when using UDM1 as reference. But taking UDM10 as reference, FUW and TS for UDM14 show significant increases of 20.7% and 74.9%, respectively. These improvements are primarily attributed to the formation of covalent bonds through the click chemistry reaction. The higher increase in TS is explained by the combination of increased FUW and decreased SAB observed for UDM14 compared to UDM10 in Figures 9 and 11. Clearly, the click chemistry reaction combined to fibrillation, compaction and the addition of 3% nanocellulose produce the best reinforcement due to the combination of all effects in a same reinforcement. However, for the FUW and considering the standard deviations in UDM11 to UDM14, it is not possible to distinguish the contribution of each individual treatment on the result. Additional analyses will be required to determine the influence of each modification. Potential influences, such as the extent to which cross-linking occurs (degree of cross-linking), the uniformity of the cross-linking throughout the material (homogeneity of cross-linking sites), and how natural fibres, which have uneven (non-isotropic) properties, respond to the formation of covalent bonds.

3.4. Tensile testing of composite plates

Figure 12 shows the standard stress-strain curves for the tensile tests conducted on the composites listed in Table 3. The well-known bilinear behavior of UD flax composites is observed for all samples. The curve starts with a first linear portion up to a strain value of approximately 0.15%, referred to as the knee of the curve. This is followed by a second linear portion beyond this point. This behavior is mainly caused by the realignment of microfibrils within the fibres [54]. In the present case, however, the tensile strain at the knee of the curve increases slightly from test to test, starting at 0.16% with C1 up to a maximum value of 0.23% for C8. These values were obtained from the intersection of slopes before and after the transient region delimiting the knee of the curve and are presented in the upper left corner of Figure 12. These results, combined with the increase in elastic modulus measured from the slopes before the knee point, suggest an extension of the elastic behavior to higher stress and strain levels. This improvement is partly attributed to an enhanced fibre-matrix interface in the composites when all treatments are applied, as in the C8 sample (plates made from UMD14 reinforcements).

As mentioned above, the fibrillation of flax fibres increases their specific surface area and combined to preform compaction, this increases fibre-fibre interactions and promotes the creation of covalent bonds between the fibres. Table 5 shows the strength, modulus of elasticity (MOE) and fracture strain (FS) for tests C1 to C8, along with percent variations compared to C1. The tensile strength of the reference composite C1 has a value of 217.1 MPa, which is consistent with the

results reported by Bernaoui et al. [12] for a unidirectional flax composite made of the same reinforcement at a V_f of 40%. Composites C2 and C3, containing fibrillated fibres only (C2) and fibrillated fibres with 3% nanocellulose (C3), exhibit mean strength increases of 10.9% and 13.2%, respectively. These improvements are relatively modest. Higher increases of 25.9 % for test C4 (C3 + compaction) and 23 % for C5 (C2 + click chemistry) were obtained. These comparable increases suggest that the effect of the click chemistry reaction alone is similar to that of preform compaction with 3% nanocellulose. Another step of amelioration is obtained when combining the click chemistry reaction to 3% Nano-OX or Nano-AZ (C6 and C7), with strength increases of 38.5 and 44.3%. The best strength properties are obtained with C8 (C7 with preform compaction before molding), with an increase in tensile strength of 53.8%. Again here, comparing tests C8 (made of the UDM14 reinforcement) and C4 (made of UDM10) allows to isolate the influence of click chemistry reaction with respect to all other treatments. Increases of 22.2% and 40.2% are observed for test C8 for the strength and MOE respectively, while the SAB is reduced by 19.4%. This is in line with the above results (Section 3.3) obtained on the dry reinforcements when comparing tests UDM14 and UDM10, where higher FUW and TS but a lower SAB were obtained for UDM14.

Globally, a continuous amelioration in strength was obtained with additional treatments, starting from fibrillation alone with C2, up to C8 comprising all treatments. These contribute 53.8% of the strength increase while click chemistry alone contributes for 22.2%. The properties of C8 are also a consequence of the propargylation and azidation of fibres, which increase their hydrophobicity and make them more compatible with the epoxy resin. This promotes the wettability of fibres and the consolidation of the interface between the fibres and the matrix, resulting in a more efficient transmission of mechanical loads [55, 56].

All samples show MOE improvements in the 16 to 50% range, except for C4 and C5 which are below 10%. Samples with the lowest MOE increases are also those with the highest increases in fracture strain. This is partly explained by the fracture strain for these samples which are the highest of all tests. The low MOE of C4, made with the UDM10 reinforcement, is consistent with the high SAB of UDM10, which was the highest of all dry reinforcements. This behavior was attributed to the presence of nanocellulose in this reinforcement. Again, this suggests that the improvements made on the SAB of the dry reinforcement is transferred to composites via higher fracture strain. For all other tests in Table 5, notable ameliorations are observed in the fracture strain, with increases between 10.1% for C8 and 14% for C3. Combined to higher MOE, higher fracture strain resulted in globally higher strengths, as also shown in Figure 12.
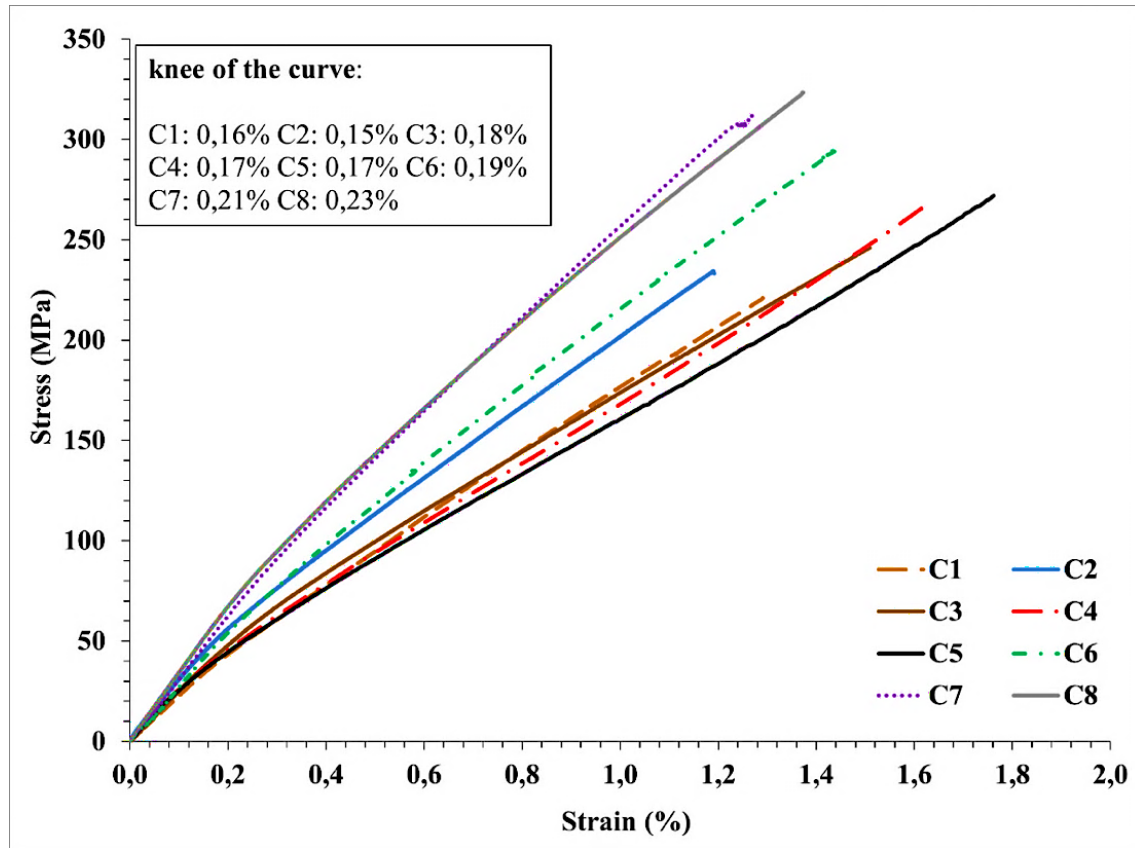
Figure 12. Typical tensile stress–strain curves for untreated and chemical treated flax fibre reinforced composites.

Table 5. Effect of treatments on the tensile properties of UDM/epoxy composites.

	Strength (MPa)	Variation. (%)	Modulus of elasticity (GPa)	Variation. (%)	Fracture strain (%)	Variation (%)
C1	217.1 ± 4.3	-	22.0 ± 1.4	-	1.28 ± 0.05	-
C2	240.7 ± 13.0	10.9	26.6 ± 2.3	20.9	1.26 ± 0.11	-1.46
C3	245.8 ± 6.2	13.2	25.4 ± 1.6	15.5	1.46 ± 0.13	13.97
C4	273.2 ± 4.1	25.9	23.6 ± 2.8	7.2	1.75 ± 0.02	36.44
C5	267.0 ± 6.7	23.0	23.9 ± 1.7	8.4	1.60 ± 0.04	24.38
C6	300.6 ± 8.1	38.5	31.2 ± 3.3	41.9	1.43 ± 0.01	11.46
C7	313.1 ± 5.8	44.3	31.8 ± 1.8	44.4	1.30 ± 0.04	1.62
C8	333.9 ± 15.1	53.8	33.1 ± 3.2	50.1	1.41 ± 0.03	10.12

Although enhancements around 50% in strength and MOE have been obtained for C8, the compaction stage and especially the presence of nanocellulose reduces the permeability to liquid resin, potentially leading to inadequate impregnation of fibre preforms. This is corroborated by the

porosity values of composites (last column of Table 3). An increase in porosity from 2.2% for C1 to 7.8% for C8 was obtained, which is quite high for composites. It is known that to minimize the composite porosity (by improving impregnation quality) during resin injection, the flow rate needs to be adjusted to balance the effect of capillary impregnation (inside fibre yarns) at low resin velocity with that of viscous forces (between reinforcement yarns) at high resin velocity [57]. The aim of the present work was not to enter into a detailed analysis of the impregnation process, but perhaps here reduced impregnation rates could improve the quality of the impregnation. However, and considering the low reinforcement permeability of UDM14 (used for plate C8), reduced impregnation rates mean longer filling times, which were not possible considering the risk of premature resin cure. Nonetheless, the actual improvements in tensile properties of C8 suggest that with lower plate porosities, properties improvements greater than 50% could be obtained. It is therefore crucial to enhance the permeability of the treated reinforcements by modifying the porous structure. This can also be done, partly at least, by optimizing the mechanical treatments, such as fibrillation and compression, as well as the chemical treatments, such as treatment duration and amounts of reagents, to improve the wettability of the fibres by the liquid resin. Finally, it is worth mentioning that the treatments were mainly designed to enhance the mechanical properties of the dry reinforcements by reinforcing fibre-fibre interactions through fibrillation, compaction, nanocellulose addition, and click chemistry. These modifications targeted mainly the internal structure of the reinforcements, focusing on fibre-fibre and nanocellulose-fibre bonds, rather than directly improving the fibre-matrix interface of the composites. As a result, the enhancements observed in the dry reinforcements, such as a 219.9 % increase in the FUW (Figure 9), are partly due to the relatively low baseline properties of the untreated reinforcements (UDM1), which amplify the percentage improvements. In composites, the baseline properties (of C1) are inherently much higher, leading to more modest improvements (around 50 %) that partly reflect the limitations imposed by the unmodified fibre-matrix interface. This distinction highlights the need for future works to focus on improving the fibre-matrix interface to fully transfer the benefits of the reinforcements' treatments to the composites. For example, click chemistry or other chemical modifications could be adapted to specifically enhance fibre-matrix bonding, thereby addressing this limitation and maximizing the mechanical performances of composites.

Figures 13 and 14 show the fracture surfaces and micrographs of C1 (untreated) and C8 (fully treated) specimens. C1 clearly shows more fibres protruding from the surface, indicating a significant fibre pull-out and poor fibre-matrix adhesion. In contrast, C8 shows a more uniform fracture surface, suggesting a stronger fibre-matrix adhesion. But as such, the increase in stiffness and strength of the reinforcement alone (without the matrix) is such that these properties are

transferred to the final composite, in addition to some improvement in the fibre-matrix interface induced by the treatments. These observations partly explain the tensile strength and fracture strain improvements (Table 5), as the series progresses from mechanical (with or without nanocellulose) to advanced chemical treatments.
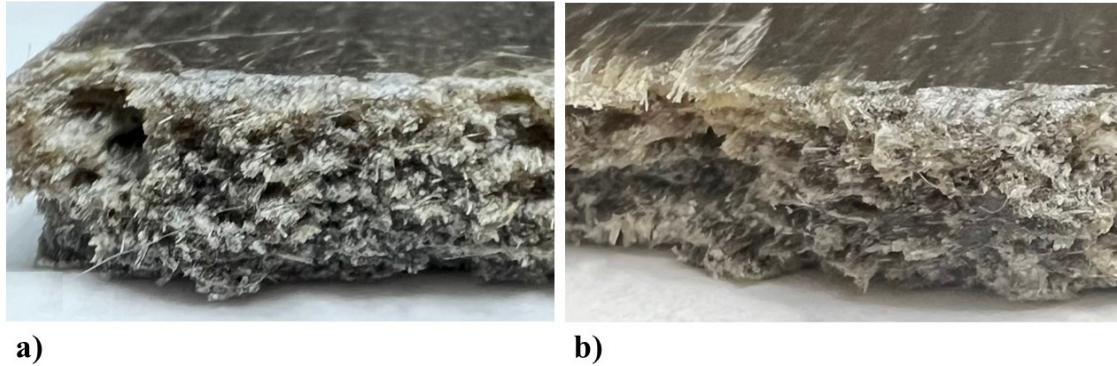

a)   b)

Figure 13. Fracture surfaces of composite specimens: a) C1 (untreated), b) C8 (fully treated).

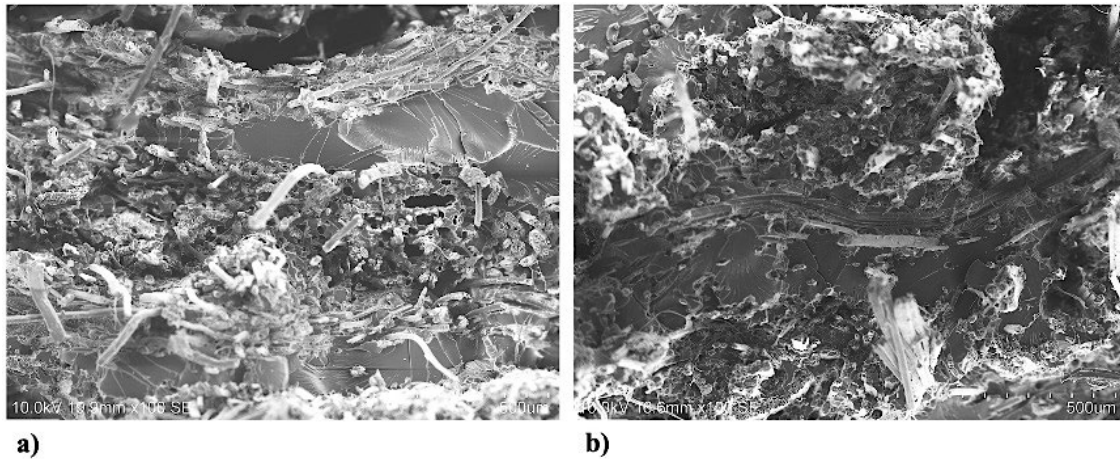a)   b)

Figure 14. SEM micrographs of fracture surfaces of composite specimens: a) C1 (untreated), b) C8 (treated).

CONCLUSION

This work focused on the application of click chemistry, combined with short fibre fibrillation, reinforcement compaction and the adding of nanocellulose, to improve the tensile properties of dry reinforcement and flax-epoxy composites obtained from UD-mat reinforcements. Fibrillation was realized to increase the accessibility of hydroxyl groups (for preliminary chemical reactions) and create mechanical interaction with the matrix. Compaction was added to potentially increase the number of covalent bonds (by increasing the number of fibre-fibre contact points) created from the

click chemistry reaction. To amplify this effect, the addition of a small amount of nanocellulose was also investigated.

The FTIR and EDX results show that the precursor treatments, i.e. propargylation, tosylation and azidation of the UD fibres, short fibres and nanocellulose, were efficiently realized with high degrees of substitution. Next, it was observed that the addition of nanocellulose strongly reduces the permeability of the reinforcements, a major drawback for liquid composite molding processes. However, adding 3% was found to be an acceptable compromise for reinforcements fabrication and plates molding. The gradual implementation of treatments, starting with fibrillation alone up to a combination of fibrillation, compaction, nanocellulose and click chemistry, results in gradual increases of the tensile strength, stiffness and strain at break of the dry reinforcements and unidirectional flax-epoxy composites. The most important increases are observed after the click chemistry reaction occurred when all mechanical treatments are applied along with nanocellulose addition to the reinforcement. Compared to the non-treated UDM1 reinforcement, increases in the tensile stiffness (+200%), strain at break (+220%), and force per unit width (+71%) of dry reinforcements confirmed the efficiency of the combined treatments. Examining the effect of click chemistry only, increases of 20.7% and 74.9% for FUW and TS respectively were obtained, confirming the influence of the crosslinking reaction.

The composites made from mechanically and chemically treated UD-mat reinforcements displayed substantial improvements in strength (+54%) and modulus of elasticity (+50%). SEM micrographs of these composites exhibited less fibre pull-out and matrix cracking, which is representative of better fibre-matrix adhesion and an efficient transfer of the dry reinforcement properties to those of the final composite. Despite these promising results, the reduced permeability caused by nanocellulose incorporation poses challenges for resin impregnation during molding. This can lead to increased porosity in the composites, which may compromise their overall performance. Additionally, the extended reaction times required to achieve high degrees of substitution represent a limitation for large volume productions of the UD-mat reinforcement at the industrial scale. Addressing these issues will require optimization, such as modifying the porous structure of the reinforcements, adjusting resin flow parameters, and exploring alternative reaction conditions to reduce process time while maintaining material performance. Moreover, the lower improvements obtained in composites (around 50 %) compared to the dry reinforcements (up to 219.9 % for the FUW) highlights the need in future work to aim at improving the fiber-matrix interface in order to fully transfer to composites the benefits of treatments performed on reinforcements. For example, click chemistry or other chemical modifications could be adapted to specifically enhance fibre-matrix bonding, thereby addressing this limitation and maximizing the mechanical performances

of composites. Nonetheless, this study clearly demonstrates the potential of combining mechanical and chemical treatments to develop higher mechanical properties for high-performance natural fibre composites used in structural applications. It also provides valuable insights into the potential of click chemistry for modifying flax fibres, enabling the creation of materials with improved properties.

ACKNOWLEDGEMENTS

REFERENCES

[1]   K. N. Keya, N. A. Kona, F. A. Koly, K. M. Maraz, M. N. Islam, and R. A. Khan, "Natural fibre reinforced polymer composites: history, types, advantages and applications," *Materials Engineering Research,* vol. 1, no. 2, pp. 69-85, 2019.

[2]   J. Zhu, H. Zhu, J. Njuguna, and H. Abhyankar, "Recent development of flax fibres and their reinforced composites based on different polymeric matrices," *Materials* vol. 6, no. 11, pp. 5171-5198, 2013.

[3]   G. Park and H. Park, "Structural design and test of automobile bonnet with natural flax composite through impact damage analysis," *Composite Structures,* vol. 184, pp. 800-806, 2018.

[4]   M. Mohammed et al., "Comprehensive insights on mechanical attributes of natural-synthetic fibres in polymer composites," *Journal of Materials Research and Technology,* vol. 25, pp. 4960–4988, 2023.

[5]   T. Sullins, S. Pillay, A. Komus, and H. Ning, "Hemp fibre reinforced polypropylene composites: The effects of material treatments," *Composites Part B: Engineering,* vol. 114, pp. 15-22, 2017.

[6]   Z. Khan, B. Yousif, and M. Islam, "Fracture behaviour of bamboo fibre reinforced epoxy composites," *Composites Part B: Engineering,* vol. 116, pp. 186-199, 2017.

[7]   M. Cai *et al.*, "Influence of alkali treatment on internal microstructure and tensile properties of abaca fibres," *Industrial Crops Products,* vol. 65, pp. 27-35, 2015.

[8]   M. Li *et al.*, "Recent advancements of plant-based natural fibre–reinforced composites and their applications," *Composites Part B: Engineering,* vol. 200, p. 108254, 2020.

[9]   T. Senthilkumar, A. K. Bharimalla, C. Sundaramoorthy, P. G. Patil, and N. Vigneshwaran, "Fibrillation of coconut fibres by mechanical refining to enhance its reinforcing potential in epoxy composites," *Fibres and Polymers,* vol. 21, pp. 2111-2117, 2020.

[10]   L. Sanchez-Echeverri, E. Ganjian, J. Medina-Perilla, G. Quintana, J. Sanchez-Toro, and M. Tyrer, "Mechanical refining combined with chemical treatment for the processing of Bamboo fibres to produce efficient cement composites," *Construction and Building Materials,* vol. 269, p. 121232, 2021.

[11]   A. Khakalo, A. Vishtal, E. Retulainen, I. Filpponen, and O. J. Rojas, "Mechanically-induced dimensional extensibility of fibres towards tough fibre networks," *Cellulose,* vol. 24, pp. 191-205, 2017.

[12]   A. Bernaoui, G. Lebrun, and E. Ruiz, "High performance natural fibre composites from mat and UD flax reinforcements backed with a mat Binder: a study of mat fibre surface fibrillation," *Composites Part A: Applied Science and Manufacturing,* vol. 160, p. 107064, 2022.

[13]   R. S. Mbakop, G. Lebrun, and F. Brouillette, "Effect of compaction parameters on preform permeability and mechanical properties of unidirectional flax fibre composites," *Composites Part B: Engineering,* vol. 176, 107083, 2019.

[14]   U. Henniges, M. Hasani, A. Potthast, G. Westman, and T. Rosenau, "Electron beam irradiation of cellulosic materials—opportunities and limitations," *Materials* vol. 6, no. 5, pp. 1584-1598, 2013.

[15]   R. Ahmad, R. Hamid, and S. Osman, "Physical and chemical modifications of plant fibres for reinforcement in cementitious composites," *Advances in Civil Engineering,* vol. 2019, 2019.

[16]   D. Thapliyal *et al.*, "Natural fibres composites: Origin, importance, consumption pattern, and challenges," *Journal of Composites Science,* vol. 7, no. 12, p. 506, 2023.

[17]   S. J. Arunachalam, R. Saravanan, and G. Anbuchezhiyan, "An overview on chemical treatment in natural fibre composites," *Materials Today: Proceedings,* 2024.

[18]   M. Zin, K. Abdan, N. Mazlan, E. Zainudin, and K. Liew, "The effects of alkali treatment on the mechanical and chemical properties of pineapple leaf fibres (PALF) and adhesion to epoxy resin," in *IOP Conference Series: Materials Science and Engineering*, vol. 368, p. 012035, 2018.

[19]   C. M. Suárez, P. R. Montejo, and O. G. Junco, "Effects of alkaline treatments on natural fibres," in *Journal of Physics: Conference Series*, vol. 2046, no. 1, p. 012056, 2021.

[20]   S. Kobayashi, K. Takada, and R. Nakamura, "Processing and characterization of hemp fibre textile composites with micro-braiding technique," *Composites part A: applied science and manufacturing,* vol. 59, pp. 1-8, 2014.

[21]   M. Pokhriyal, P. K. Rakesh, S. M. Rangappa, and S. Siengchin, "Effect of alkali treatment on novel natural fibre extracted from Himalayacalamus falconeri culms for polymer composite applications," *Biomass Conversion and Biorefinery,* pp. 1-17, 2023.

[22]   A. Ali *et al.*, "Hydrophobic treatment of natural fibres and their composites—A review," *Journal of Industrial Textiles,* vol. 47, no. 8, pp. 2153-2183, 2018.

[23]   C. Taek-Jun *et al.*, "The Improvement of Mechanical Properties, Thermal Stability, and Water Absorption Resistance of an Eco-Friendly PLA/Kenaf Biocomposite Using Acetylation," *Applied Sciences,* vol. 8, no. 3, 2018.

[24]   H. Al Abdallah, B. Abu-Jdayil, and M. Z. Iqbal, "Improvement of mechanical properties and water resistance of bio-based thermal insulation material via silane treatment," *Journal of Cleaner Production,* vol. 346, p. 131242, 2022.

[25]   Y. Xie, C. A. S. Hill, Z. Xiao, H. Militz, and C. Mai, "Silane coupling agents used for natural fiber/polymer composites: A review," *Composites Part A: Applied Science and Manufacturing*, vol. 41, no. 7, pp. 806–819, Mar. 2010.

[26]   S. Alix, L. Lebrun, C. Morvan, and S. Marais, "Study of water behaviour of chemically treated flax fibres-based composites: A way to approach the hydric interface," *Composites Science and Technology,* vol. 71, no. 6, pp. 893-899, 2011.

[27]   J. Tengsuthiwat, U. Asawapirom, S. Siengchin, and J. Karger-Kocsis, "Mechanical, thermal, and water absorption properties of melamine–formaldehyde-treated sisal fibre containing poly (lactic acid) composites," *Journal of Applied Polymer Science,* vol. 135, no. 2, p. 45681, 2018.

[28]   S. Y. Nayak, S. S. Heckadka, A. Seth, S. Prabhu, R. Sharma, and K. R. Shenoy, "Effect of chemical treatment on the physical and mechanical properties of flax fibres: A comparative assessment," *Materials Today: Proceedings,* vol. 38, pp. 2406-2410, 2021.

[29]   Z. Zulyadain, J. M. Yelwa, S. Abdullahi, I. U. Gwangwazo, and O. Ojo, "Effect of Benzoyl Chloride and Fibre Loading on Mechanical Properties and Biodegradation of Poly Lactic Acid/Sugarcane Bagasse Fibre Composites," *European Journal of Applied Science, Engineering and Technology,* vol. 1, no. 1, pp. 38-52, 2023.

[30]   S. F. K. Sherwani, M. S. B. Salit, E. S. b. Zainudin, Z. Leman, and A. Khalina, "Physical and flammability properties of treated sugar palm fibre reinforced polylactic acid composites," *Journal of Industrial Textiles,* vol. 52, 2022.

[31]   W. Jordan and P. Chester, "Improving the properties of banana fibre reinforced polymeric composites by treating the fibres," *Procedia engineering,* vol. 200, p. 283-289, 2017.

[32]   W. Wang *et al.*, "Surface modification of flax fibres with isocyanate and its effects on fibre/epoxy interfacial properties," *Fibres and Polymers* vol. 21, p. 2888-2895, 2020.

[33]   F. Khan *et al.*, "Advances of Natural Fibres Composites in Diverse Engineering Applications–A Review," *Applications in Engineering Science,* p. 100184, 2024.

[34]   R. Verma, M. Shukla, and D. K. Shukla, "A treatise on mechanical properties of natural and synthetic fibre reinforced hybrid polymer composites," *Materials Today: Proceedings,* vol. 106, p. 177-183, 2024.

[35]   H. Sharma *et al.*, "Critical review on advancements on the fibre-reinforced composites: Role of fibre/matrix modification on the performance of the fibrous composites," *Journal of Materials Research and Technology,* vol.26, p. 2975-3002, 2023.

[36]   M. A. Azka, S. Sapuan, H. Abral, E. Zainudin, and F. A. Aziz, "An examination of recent research of water absorption behavior of natural fibre reinforced polylactic acid (PLA) composites: A review," *International journal of biological macromolecules,* vol. 268, p. 131845, 2024.

[37]   X. Meng, Y. Dong, W. Tan, Y. Xia, and L. Liang, "Click-based Chemical Modification of Cotton Fabric and Its Oil/Water Separation Application," *Journal of Natural Fibres,* vol. 19, no. 14, pp. 8738-8749, 2022.

[38]   X. Zhang, S. Zhang, S. Zhao, X. Wang, B. Liu, and H. Xu, "Click chemistry in natural product modification," *Frontiers in Chemistry,* vol. 9, p. 774977, 2021.

[39]   M. Wang *et al.*, "Chemical grafting of nano-SiO2 onto graphene oxide via thiol-ene click chemistry and its effect on the interfacial and mechanical properties of GO/epoxy composites," *Composites Science and Technology,* vol. 182, p. 107751, 2019.

[40]   Z. Geng, J. J. Shin, Y. Xi, and C. J. Hawker, "Click chemistry strategies for the accelerated synthesis of functional macromolecules," Journal of Polymer Science, vol. 59, no. 11, pp. 963–1042, 2021.

[41]   B. Zhang, Z. Li, and L. Wang, "Novel design and fabrication of form-stable cellulose nanofibre-based phase change composites via click chemistry, coordination reaction, and solvent exchange," *Chemical Engineering Journal,* vol. 471, p. 144417, 2023.

[42]   A. Blal, F. Brouillette, É. Loranger, and G. Lebrun, "Click chemistry modifications for the selective crosslinking of wood pulp fibres–effect on the physical and mechanical properties of paper," *RSC advances,* vol. 14, no. 14, pp. 9656-9667, 2024.

[43]   A. Blal, G. Lebrun, F. Brouillette, and É. Loranger, "Enhancement of tensile properties of flax-mat epoxy composites via click chemistry with surface fibrillation and compaction of the fiber preforms," *Journal of Materials Science*, vol. 60, p. 5080-5105, March 2025.

[44]   K.-Y. Lee, Y. Aitomäki, L. A. Berglund, K. Oksman, and A. Bismarck, "On the use of nanocellulose as reinforcement in polymer matrix composites," *Composites Science and Technology,* vol. 105, pp. 15-27, 2014.

[45]   A. Jabbar, J. Militký, J. Wiener, B. M. Kale, U. Ali, and S. Rwawiire, "Nanocellulose coated woven jute/green epoxy composites: Characterization of mechanical and dynamic mechanical behavior," *Composite Structures,* vol. 161, pp. 340-349, 2017.

[46]   E. Ameri, G. Lebrun, and L. Laperrière, "A Novel Process for the Production of Unidirectional Hybrid Flax/Paper Reinforcement for Eco-composite Materials," *Procedia CIRP,* vol. 17, pp. 778–782, 2014.

[47]   M. Habibi, L. Laperrière, G. Lebrun, and L. Toubal, "Combining short flax fibre mats and unidirectional flax yarns for composite applications: Effect of short flax fibres on biaxial mechanical properties and damage behaviour," *Composites. Part B, Engineering,* vol. 123, pp. 165–178, 2017.

[48]   R. S. Mbakop, G. Lebrun, and F. Brouillette, "Experimental analysis of the planar compaction and preforming of unidirectional flax reinforcements using a thin paper or flax mat as binder for the UD fibres," *Composites. Part a, Applied Science and Manufacturing,* vol. 109, pp. 604–614, 2018.

[49]   M. Lassoued, F. Crispino, and E. Loranger, "Design and synthesis of transparent and flexible nanofibrillated cellulose films to replace petroleum-based polymers," *Carbohydrate Polymers,* vol. 254, p. 117411, 2021.

[50]   M. L. Gall, P. Davies, N. Martin, and C. Baley, "Recommended flax fibre density values for composite property predictions," *Industrial Crops and Products,* vol. 114, pp. 52–58, 2018.

[51]   A. Amiri, Z. Triplett, A. Moreira, N. Brezinka, M. Alcock, and C. A. Ulven, "Standard density measurement method development for flax fibre," *Industrial Crops and Products,* vol. 96, pp. 196–202, 2016.

[52]   K. L. Adams and L. Rebenfeld, "In-Plane Flow of Fluids in Fabrics: Structure/Flow Characterization," *Textile Research Journal,* vol. 57, no. 11, pp. 647–654, 1987.

[53] L. Mishnaevsky, L. P. Mikkelsen, A. N. Gaduan, K.-Y. Lee, and B. Madsen, "Nanocellulose reinforced polymer composites: Computational analysis of structure-mechanical properties relationships," *Composite Structures,* vol. 224, p. 111024, 2019.

[54] L. Yan, N. Chouw, and K. Jayaraman, "Flax fibre and its composites – A review," *Composites Part B: Engineering,* vol. 56, pp. 296–317, 2014.

[55] N. S. A. Rahman, N. A. Ahmad, M. F. Yhaya, B. Azahari, and W. R. Ismail, "Crosslinking of fibres via azide–alkyne click chemistry: Synthesis and characterization," *Journal of Applied Polymer Science,* vol. 133, no. 25, 2016.

[56] F. Wang, M. Lu, S. Zhou, Z. Lu, and S. Ran, "Effect of Fibre Surface Modification on the Interfacial Adhesion and Thermo-Mechanical Performance of Unidirectional Epoxy-Based Composites Reinforced with Bamboo Fibres," Molecules/Molecules Online/Molecules Annual, vol. 24, no. 15, p. 2682, 2019.

[57] E. Ruiz, V. Achim, S. Soukane, F. Trochu, and J. Breard, "Optimization of injection flow rate to minimize micro/macro-voids formation in resin transfer molded composites," *Composites Science and Technology*, vol. 66, no. 3–4, pp. 475–486, 2005.